

TRIANGULAR AND TETRAHEDRAL SPACE-TIME FINITE ELEMENTS IN VIBRATION ANALYSIS

CZESŁAW I. BAJER

Department of Civil Engineering, Engineering College, Podgórna 50, 65-246 Zielona Góra, Poland

SUMMARY

Recently, several methods of time integration of the equations of motion have been proposed. Many of them result in square mass, damping and stiffness matrices. The space-time finite element method is an extension of the FEM, familiar to most engineers, over the time domain. A special approach enables the use of triangular, tetrahedral and hyper-tetrahedral elements in time and space. By special division of the space-time layer the triangular matrix of coefficients in the system of equations can be obtained. A simple algorithm enables the storage of non-zero coefficients only. Dynamic solution requires a small amount of the memory compared to other methods, and ensures considerable reduction of arithmetic operations. The method presented is also efficient in solving both linear and non-linear problems. Matrices for a beam and plane stress/strain element are derived. Exemplary problems solved by the method described have proved the effectiveness of the application of triangular and tetrahedral space-time elements in vibration analysis.

INTRODUCTION

Discrete methods enable modelling of complicated problems in structural engineering. However, approximation requirements result in matrix equations with many degrees of freedom. In cases of dynamic and non-linear problems the significant increase of costs has stimulated the growth of research directed towards the development of algorithms designed for these problems. There are two general classes of algorithms: implicit and explicit. Implicit algorithms permit large time steps, but the cost of one step of computations is high, and storage requirements increase considerably with the size of the mesh. Implicit methods can be considered as numerically stable ones. On the other hand, the explicit methods are inexpensive, considering the number of operations per step, and require less storage than implicit ones. The stability restrictions usually require small time steps, making the computations more expensive. Mixed implicit-explicit methods which include the best features of both types of algorithms have also been worked out. Both implicit and explicit methods described in the literature have many disadvantages. In each algorithm for the integration of the equation of motion the stiff partition into finite elements is assumed. In linear problems the stiffness, mass and damping matrices are computed once at the beginning and they are valid throughout each step. In non-linear problems the matrices are computed using the same mesh as initially assumed. The stationary division of the construction enables the solution of some essential problems. For example, vibrations of a structure with travelling support can be solved only if a non-stationary division is assumed. A partition varying at each step is also useful in plastic region approximation, in contact problems, movable, edge problems etc.

The second disadvantage of the method developed to date is more general and concerns the

solution of the system of equations. The matrices obtained in the computations are square and banded. The final coefficient matrix has the same form. Even in the case of optimum numbering of the mesh nodes the efficient solution requires holding the square part of the band in the memory. Then, the matrix can be effectively triangularized with the use of external memory. Although in linear problems with constant coefficients such a procedure can be applied once even by the use of a time consuming method, in problems with variable coefficients the proper memory must be permanently provided. Since the computations in vibration analysis are carried out many times, in order to provide efficiency they should be performed in core. This is the reason why the size of the structure analysed depends so strongly on the size of the computer memory.

The third problem concerns the possibility of decreasing the time step in regions of high speed of displacements. It can be achieved by a mixed implicit–explicit method,^{1–3} in which the implicit method is applied in one spatial region whereas the explicit one is used in the other.

Several papers have elaborated on finite element analysis in the time domain. New integration methods have been proposed^{4,5} and an efficient method has been described.⁶ However, to allow the element-by-element procedure a diagonal mass matrix must be assumed. A comparative analysis has been performed.⁷ A broad survey of the state of the art in the field of finite element application to dynamic problems has been given⁸ and an introduction into the space-time element technology has been described.⁹ Unfortunately, in none of these papers is there an approach which provides easy manipulation of finite elements in time. This is why some serious practical problems cannot be simply solved. The space–time finite element method (STFEM), of which some aspects will be described below, can be regarded as an extension of common finite elements over the time domain.^{10–13} The easiness of the time–space partition, almost as easy as the spatial discretization, makes the method useful in the solution of problems with movable edges. All the disadvantages mentioned previously can now be overcome. In this paper, time–space partition into triangular, tetrahedral and hyper-tetrahedral space–time finite elements will be discussed and benefits in the computational process will be exhibited. Considerable reduction of the matrix form and savings in arithmetical calculations are not the only values of the application described. This paper is limited to the basic applicable properties of the method, but since the STFEM is similar to the FEM familiar to most engineers wider applications are imaginable. In the present formulation the method is conditionally stable. This is not so strong a restriction in cases of geometrically non-linear problems, for which the method is particularly comfortable.

OUTLINE OF THE SPACE–TIME FINITE ELEMENT THEORY

The space–time finite element can be understood as a finite element in which the additional time dimension is considered. Therefore, the space–time system of elements has more dimensions. For example, a beam element has rectangular shape and a plate element becomes a three-dimensional rectangular prism (Figure 1(a)). Non-rectangular space–time elements are also possible (Figure 1(b)). To clarify further considerations the basic principles of the method will be included.

Let \mathbf{f} be a displacement vector at any point of the element volume. It can be expressed in terms of the nodal values δ_e

$$\mathbf{f} = \mathbf{N}\delta_e \quad (1)$$

\mathbf{N} is the matrix of the shape functions. The stress $\boldsymbol{\sigma}$ and strain $\boldsymbol{\varepsilon}$ can be expressed by the commonly known relations (the Kelvin–Voigt model was assumed)

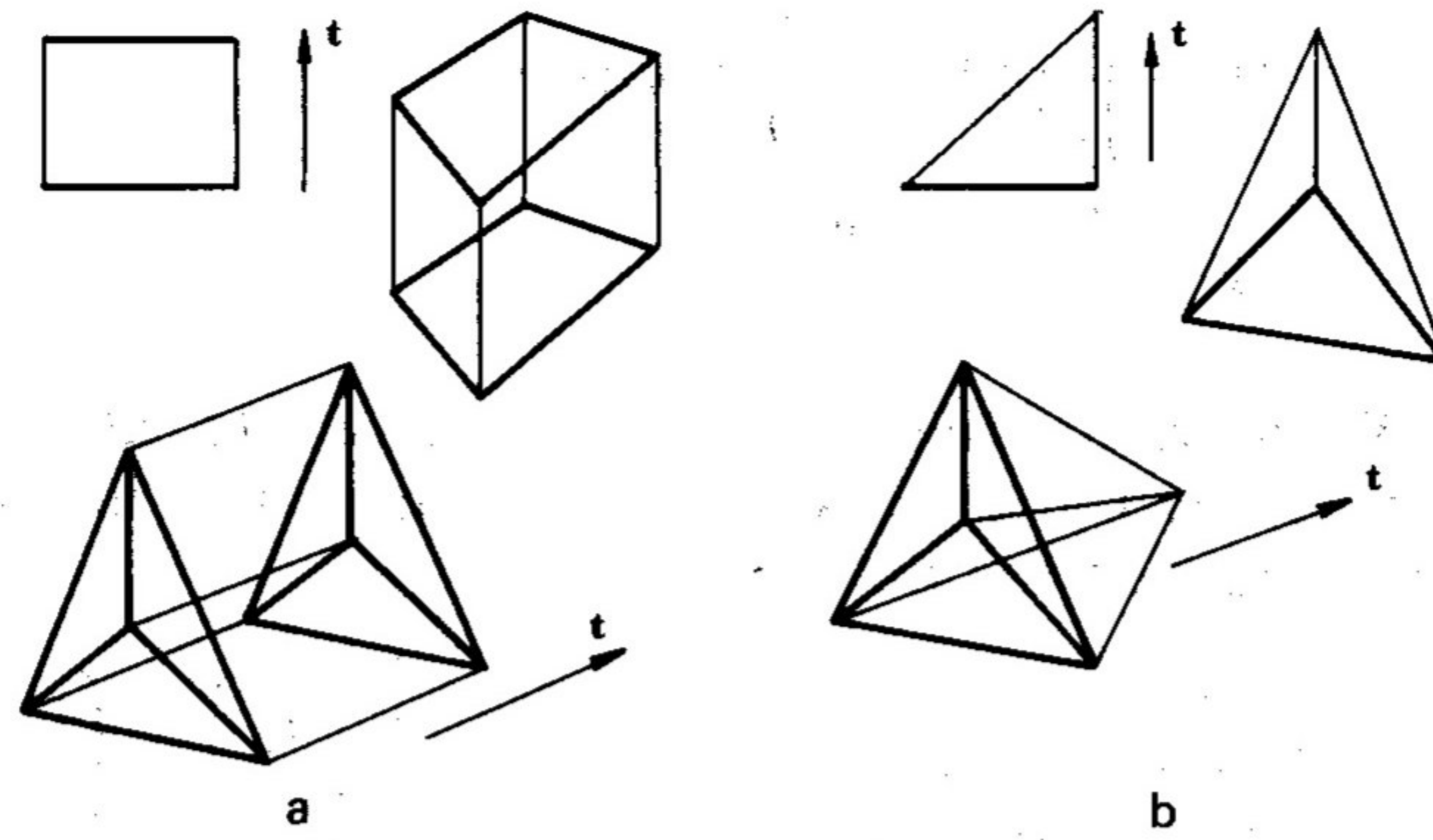


Figure 1. Rectangular and non-rectangular space-time finite elements

$$\epsilon = \partial_x \mathbf{f} = \partial_x \mathbf{N} \delta_e \tag{2}$$

$$\sigma = \left(\mathbf{E} + \eta_w \frac{\partial}{\partial t} \right) \epsilon \tag{3}$$

∂_x is the matrix of differential operators, \mathbf{E} is the matrix of the elasticity constants and η_w is a coefficient of internal damping. Deformation of the element in time ϵ_t can be determined as a velocity

$$\epsilon_t = \frac{\partial \mathbf{f}}{\partial t} = \frac{\partial \mathbf{N}}{\partial t} \delta_e \tag{4}$$

The momentum of the material point is

$$\sigma_t = -\mathbf{R} \epsilon_t \tag{5}$$

\mathbf{R} denotes the matrix of elementary inertia coefficients. Denoting η_z as an external damping coefficient, the virtual four-work of internal forces in the volume of the element can be equated to the four-work of external forces

$$\int_V (\delta \epsilon^T \sigma + \delta \epsilon_t^T \sigma_t) dV = \delta \delta_e F_e - \int_V \delta \mathbf{f}^T \eta_z \frac{\partial \mathbf{f}}{\partial t} dV \tag{6}$$

Considering (2)–(5) it can be written that

$$\int_V \left[(\partial_x \mathbf{N})^T \mathbf{E} \partial_x \mathbf{N} + (\partial_x \mathbf{N})^T \eta_w \frac{\partial}{\partial t} \partial_x \mathbf{N} - \left(\frac{\partial}{\partial t} \mathbf{N} \right)^T \mathbf{R} \frac{\partial}{\partial t} \mathbf{N} + \mathbf{N}^T \eta_z \frac{\partial}{\partial t} \mathbf{N} \right] dV \delta_e = F_e \tag{7}$$

For the whole construction the following matrix equation can be obtained:

$$(\mathbf{K} + \mathbf{M} + \mathbf{W} + \mathbf{Z}) \delta = \mathbf{F} \tag{8}$$

or

$$\mathbf{K}^* \delta = \mathbf{F} \tag{9}$$

where

$$\mathbf{K} = \int_V (\partial_x \mathbf{N})^T \mathbf{E} \partial_x \mathbf{N} dV \tag{10}$$

$$\mathbf{M} = - \int_V \left(\frac{\partial}{\partial t} \mathbf{N} \right)^T \mathbf{R} \frac{\partial}{\partial t} \mathbf{N} dV \tag{11}$$

$$\mathbf{W} = \int_V (\partial_x \mathbf{N})^T \eta_w \frac{\partial}{\partial t} \partial_x \mathbf{N} dV \quad (12)$$

$$\mathbf{Z} = \int_V \mathbf{N}^T \eta_z \frac{\partial \mathbf{N}}{\partial t} dV \quad (13)$$

The matrices \mathbf{K} , \mathbf{M} , \mathbf{W} and \mathbf{Z} are called the stiffness, mass, internal damping and external damping matrices, respectively. The analysis of the joint connections in several successive time layers leads to the global matrix \mathbf{K}^* in the form

$$\begin{bmatrix} \mathbf{A}_1 & \mathbf{B}_1 & & & & \\ \mathbf{C}_1 & \mathbf{D}_1 + \mathbf{A}_2 & \mathbf{B}_2 & & & \\ & \mathbf{C}_2 & \mathbf{D}_2 + \mathbf{A}_3 & \mathbf{B}_3 & & \\ & & \mathbf{C}_3 & \mathbf{D}_3 + \mathbf{A}_4 & \cdot & \\ & & & & \cdot & \\ & & & & & \cdot \end{bmatrix} \begin{Bmatrix} \delta_1 \\ \delta_2 \\ \delta_3 \\ \delta_4 \\ \vdots \end{Bmatrix} = \begin{Bmatrix} \mathbf{F}_1 \\ \mathbf{F}_2 \\ \mathbf{F}_3 \\ \mathbf{F}_4 \\ \vdots \end{Bmatrix} \quad (14)$$

i.e. for one time layer equation (9) has the form

$$\mathbf{C}_{i-1} \delta_{i-1} + (\mathbf{D}_{i-1} + \mathbf{A}_i) \delta_i + \mathbf{B}_i \delta_{i+1} = \mathbf{F}_i \quad (15)$$

Such a formulation enables step-by-step solution. The dimensions of the submatrices \mathbf{A}_i , \mathbf{B}_i , \mathbf{C}_i and \mathbf{D}_i are equal to the total number of degrees of freedom related to the entire structure. In this meaning the space-time finite element method can be regarded as a time integration method. However, the time-space region can be divided into space-time elements of almost any shape. Although some restrictions are imposed on the shape, in practical use the arbitrary time-space division can be applied.

Triangular element of a beam (first model)

The assumption of a linear distribution of displacements in the space-time element enables the simple derivation of the stiffness, mass and damping matrices. Let the deflection w and the angle of rotation θ be given by linear relations

$$\begin{Bmatrix} w \\ \theta \end{Bmatrix} = \begin{Bmatrix} a_1 x + a_2 t + a_3 \\ b_1 x + b_2 t + b_3 \end{Bmatrix} = \begin{Bmatrix} \mathbf{a} \mathbf{g} \\ \mathbf{b} \mathbf{g} \end{Bmatrix} \quad (16)$$

where

$$\mathbf{g} = [x, t, 1] \quad (17)$$

and \mathbf{a} , \mathbf{b} contain the constants a_i , b_i , $i = 1, 2, 3$. Denoting by \mathbf{r}_i the columns of the inverted matrix of nodal co-ordinates

$$\mathbf{G}^{-1} = \begin{bmatrix} x_1 & t_1 & 1 \\ x_2 & t_2 & 1 \\ x_3 & t_3 & 1 \end{bmatrix}^{-1} = [\mathbf{r}_1, \mathbf{r}_2, \mathbf{r}_3] \quad (18)$$

the shape matrix \mathbf{N} can be determined:

$$\mathbf{N} = [\mathbf{N}_1, \mathbf{N}_2, \mathbf{N}_3], \quad \mathbf{N}_i = \mathbf{g} \mathbf{r}_i \begin{bmatrix} 1 & 0 \\ 0 & 1 \end{bmatrix} \quad (19)$$

In the case of a beam, the differential operator ∂_x has the form

$$\partial_x = \begin{bmatrix} \frac{\partial}{\partial x} & 1 \\ 0 & \frac{\partial}{\partial x} \end{bmatrix} \quad (20)$$

The elasticity matrix is

$$\mathbf{E} = \text{diag} \left[\frac{GA}{K}, EI \right] \quad (21)$$

where G is the shear modulus, A is the area of the cross-section, K is the shape factor for the cross-section and EI is the flexural stiffness. The elementary inertia matrix is

$$\mathbf{R} = \text{diag} [\rho A, \rho I] \quad (22)$$

Considering relations (10)–(13) one can compute the matrices \mathbf{K} , \mathbf{M} , \mathbf{W} and \mathbf{Z} . The integration over the element volume can be accomplished analytically if the origin of co-ordinates is placed at the centre of gravity of the element. Then, after addition according to (8) the stiffness matrix \mathbf{K}^* can be written

$$\mathbf{K}_{ij}^* = \begin{bmatrix} \frac{GA}{4KV} (t_k - t_l)(t_m - t_n) - \frac{\rho A}{4V} (x_k - x_l)(x_m - x_n) & \frac{GA}{4KV} (t_k - t_l)(x_m t_n - x_n t_m) + \frac{\eta_w}{4V} (t_k - t_l)(x_n - x_m) \\ + \frac{\eta_z}{4V} (x_k t_l - x_l t_k)(x_n - x_m) & \\ \frac{GA}{4KV} (t_m - t_n)(x_k t_l - x_l t_k) & \frac{EI}{4V} (t_k - t_l)(t_m - t_n) - \frac{\rho I}{4V} (x_k - x_l)(x_m - x_n) \\ & + \frac{\eta_w + \eta_z}{4V} (x_k t_l - x_l t_k)(x_n - x_m) \end{bmatrix} \quad (23)$$

where V is the volume of the element and x_i, t_i are the nodal co-ordinates. The indices are changed periodically in a sequence i, k, l and j, m, n .

Triangular element of a beam (second model)

To form correctly formulated shape functions we must ensure the conformance of the displacements on the edges of neighbouring elements. The assumption of a displacement distribution varying cubically along the element sides allows the evaluation of displacements at an additional 6 mid-side nodes. Then a polynomial of sufficiently high order can be assumed to express the displacement distribution in the element area. The displacements on the edges are expressed in terms of the nodal values by the form

$$\mathbf{f}_k = \begin{Bmatrix} w \\ \theta \end{Bmatrix} = \mathbf{N}_1^k \delta_i + \mathbf{N}_2^k \delta_j = \mathbf{f}_k(\xi) \quad (24)$$

in which δ_i, δ_j represent the nodal displacements and \mathbf{N}_i^k is the matrix of cubic and quadratic

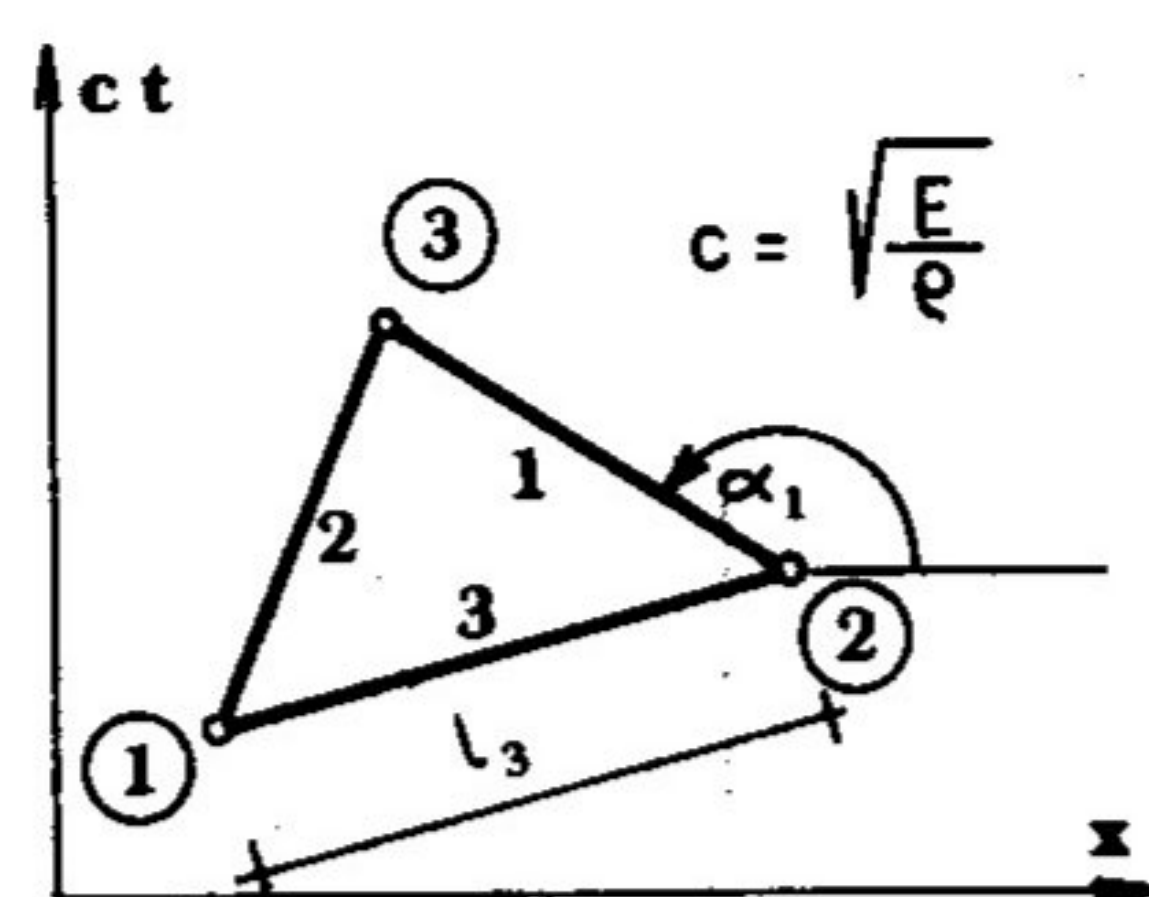


Figure 2. Triangular space-time element

relations describing the displacements on the edge k . The expressions N_i^k are related to the co-ordinate ξ as follows

$$\mathbf{N}_i^k = \begin{bmatrix} N_{11i} & N_{12i} \\ N_{21i} & N_{22i} \end{bmatrix} \quad (25)$$

$$\begin{aligned} N_{11i} &= m_1 - \mu m_3 \cos^2 \alpha_k \\ N_{12i} &= \frac{1}{2} \xi_i l_k (m_2 - \mu m_3) \cos \alpha_k \\ N_{21i} &= -\xi_i m_1^{(1)} (1 - \mu) \frac{2}{l_k} \cos \alpha_k \\ N_{22i} &= -(m_2^{(1)} - \mu m_1^{(1)}) \cos^2 \alpha_k + \frac{1}{2} (1 + \xi \xi_i) \sin^2 \alpha_k \end{aligned} \quad (26)$$

where

$$\mu = \frac{3\gamma}{1 + 3\gamma}, \quad \gamma = \frac{EIK}{GA \left(\frac{\partial x}{\partial \xi} \right)^2} \quad (27)$$

The length of the side k , denoted by l_k , and the angle between the axis Ox and the edge k of the triangle α_k are shown in Figure 2. The polynomials m_1 , m_2 , m_3 and their derivatives are

$$\begin{aligned} m_1 &= 0.25(-\xi_0^3 + 3\xi_0 + 2), & m_1^{(1)} &= 0.75(-\xi_0^2 + 1) \\ m_2 &= 0.25(-\xi_0^3 - \xi_0^2 + \xi_0 + 2), & m_2^{(1)} &= 0.25(-3\xi_0^2 - 2\xi_0 + 1) \\ m_3 &= 0.25(-\xi_0^3 + \xi_0), & \xi_0 &= \xi \xi_i \end{aligned} \quad (28)$$

The distribution of displacements inside the element is expressed by the polynomials

$$\mathbf{f}(x, t) = \begin{Bmatrix} w \\ \theta \end{Bmatrix} = \begin{Bmatrix} a_1 x^3 + a_2 (x^2 t + x t^2) + a_3 t^3 + a_4 x^2 + a_5 x t + a_6 t^2 + a_7 x + a_8 t + a_9 \\ b_1 x^3 + b_2 (x^2 t + x t^2) + b_3 t^3 + b_4 x^2 + b_5 x t + b_6 t^2 + b_7 x + b_8 t + b_9 \end{Bmatrix} \quad (29)$$

Let us define vectors \mathbf{a} and \mathbf{b} as sequences of unknown coefficients a_1, \dots, a_9 and b_1, \dots, b_9 , respectively, and let the vector \mathbf{g} be of the form

$$\mathbf{g} = [x^3, x^2 t + x t^2, t^3, x^2, x t, t^2, x, t, 1] \quad (30)$$

The displacements w at all nine nodes, denoted by w_e , can be expressed by the relation

$$\mathbf{w}_e = \begin{bmatrix} \mathbf{g}(x_1, t_1) \\ \mathbf{g}(x_2, t_2) \\ \vdots \\ \mathbf{g}(x_9, t_9) \end{bmatrix} \mathbf{a} = \mathbf{G} \mathbf{a} \quad (31)$$

and the displacements θ at the nine nodes, denoted by θ_e , by the relation

$$\theta_e = Gb \quad (32)$$

Then the unknown \mathbf{a} and \mathbf{b} can be evaluated by the inversion of \mathbf{G} in (31) and (32). Nodal values of w_e and θ_e must be computed by multiplication of the vector δ_e by the matrices \mathbf{A}_w and \mathbf{A}_θ , respectively. Coefficients of the matrices \mathbf{A}_w and \mathbf{A}_θ should be found to express displacements at the nine nodes in terms of three main joint displacements

$$w_e = \mathbf{A}_w \delta_e, \quad \theta_e = \mathbf{A}_\theta \delta_e \quad (33)$$

The shape functions are given by

$$\mathbf{N}(x, t) = \begin{bmatrix} \mathbf{g}(x, t) & \mathbf{G}^{-1} & \mathbf{A}_w \\ \mathbf{g}(x, t) & \mathbf{G}^{-1} & \mathbf{A}_\theta \end{bmatrix} \quad (34)$$

The differentiations in relations (10)–(13) can be performed as follows:

$$\partial_x \mathbf{N} = \frac{\partial \mathbf{g}(x, t)}{\partial x} \mathbf{G}^{-1} \begin{bmatrix} \mathbf{A}_w \\ \mathbf{A}_\theta \end{bmatrix} + \mathbf{g}(x, t) \mathbf{G}^{-1} \begin{bmatrix} \mathbf{A}_\theta \\ \mathbf{0} \end{bmatrix} \quad (35)$$

$$\frac{\partial \mathbf{N}}{\partial t} = \frac{\partial \mathbf{g}(x, t)}{\partial t} \mathbf{G}^{-1} \begin{bmatrix} \mathbf{A}_w \\ \mathbf{A}_\theta \end{bmatrix} \quad (36)$$

$$\frac{\partial}{\partial t} \partial_x \mathbf{N} = \frac{\partial^2 \mathbf{g}(x, t)}{\partial x \partial t} \mathbf{G}^{-1} \begin{bmatrix} \mathbf{A}_w \\ \mathbf{A}_\theta \end{bmatrix} \quad (37)$$

Tetrahedral element of plane stress/strain

Let us assume a linear distribution of displacements \mathbf{f} in the element

$$\mathbf{f}(x, y, t) = \begin{bmatrix} u \\ v \end{bmatrix} = \begin{bmatrix} \mathbf{g} & \mathbf{a} \\ \mathbf{g} & \mathbf{b} \end{bmatrix} \quad (38)$$

where

$$\mathbf{g} = [x, y, t, 1] \quad (39)$$

and \mathbf{a} , \mathbf{b} are the vectors of four constants a_i , b_i , $i = 1, 2, 3, 4$. Then, if the columns of the matrix \mathbf{G}^{-1} are denoted by $\mathbf{r}_i = [p_{1i}, p_{2i}, p_{3i}, p_{4i}]^T$, the shape matrix \mathbf{N} has the form

$$\mathbf{N} = [\mathbf{N}_1, \mathbf{N}_2, \mathbf{N}_3, \mathbf{N}_4], \quad \mathbf{N}_i = \mathbf{g} \mathbf{r}_i \begin{bmatrix} 1 & 0 \\ 0 & 1 \end{bmatrix} \quad (40)$$

The matrix ∂_x used in (2) for the case of plane stress and the matrix \mathbf{E} used in (3) are well known:

$$\partial_x = \begin{bmatrix} \frac{\partial}{\partial x} & 0 \\ 0 & \frac{\partial}{\partial y} \\ \frac{\partial}{\partial y} & \frac{\partial}{\partial x} \end{bmatrix}, \quad \mathbf{E} = \frac{E}{1-\nu^2} \begin{bmatrix} 1 & \nu & 0 \\ \nu & 1 & 0 \\ 0 & 0 & \frac{1-\nu}{2} \end{bmatrix} \quad (41)$$

where E is Young's modulus and ν is Poisson's ratio.

The inertia matrix \mathbf{R} is diagonal with elements equal to the mass density ρ .

To simplify the integration over the volume V let us assume the nodal co-ordinates which satisfy the relations

$$\sum x_i = 0, \quad \sum y_i = 0, \quad \sum t_i = 0 \tag{42}$$

The submatrices \mathbf{K}_{ij} , \mathbf{M}_{ij} , \mathbf{W}_{ij} and \mathbf{Z}_{ij} can be written

$$\mathbf{K}_{ij} = V \begin{bmatrix} \frac{E}{1-\nu^2} p_{1i} p_{1j} + \frac{E}{2(1+\nu)} p_{2i} p_{2j} & \frac{E}{1-\nu^2} p_{1i} p_{2j} + \frac{E}{2(1+\nu)} p_{2i} p_{1j} \\ \frac{E}{1-\nu^2} p_{2i} p_{1j} + \frac{E}{2(1+\nu)} p_{1i} p_{2j} & \frac{E}{1-\nu^2} p_{2i} p_{2j} + \frac{E}{2(1+\nu)} p_{1i} p_{1j} \end{bmatrix} \tag{43}$$

$$\mathbf{M}_{ij} = -\rho V p_{3i} p_{3j} \mathbf{I} \tag{44}$$

$$\mathbf{W}_{ij} = \mathbf{0} \tag{45}$$

$$\mathbf{Z}_{ij} = \eta_z V p_{4i} p_{3j} \tag{46}$$

\mathbf{I} denotes the 2×2 unit matrix and $\mathbf{0}$ the 2×2 zero matrix. In plane strain analysis the matrix \mathbf{E} (41) must be replaced by the appropriate form. It is seen from equation (45) that in the case of low polynomial order internal damping cannot be considered.

SOLUTION ALGORITHM

If the stationary division was assumed, the algorithm could be considered as an integration method for the equation of motion. It could be considered as an explicit time integration method. Global matrices of the system of equations (15) related to one time-space layer were filled by non-zero elements in the way resulting from the division of the construction into finite elements and the numbering of joints. Non-zero elements were placed symmetrically. The evaluation of joint displacements at the given moment required the solution of the system of equations. The mesh condensation caused the matrix band widening, along with increasing the total number of equations. In the presented algorithm triangular, tetrahedral and hyper-tetrahedral elements are of the special interest. The application of the elements depicted in Figure 1(b) enables us to gain the triangular coefficient matrices of the system of equations (15) under the condition of a special numbering of the nodes. Figure 3 presents a space-time layer in the case of a unidimensional structure and the global stiffness matrix \mathbf{K}^* from equations (8) and (9). The right

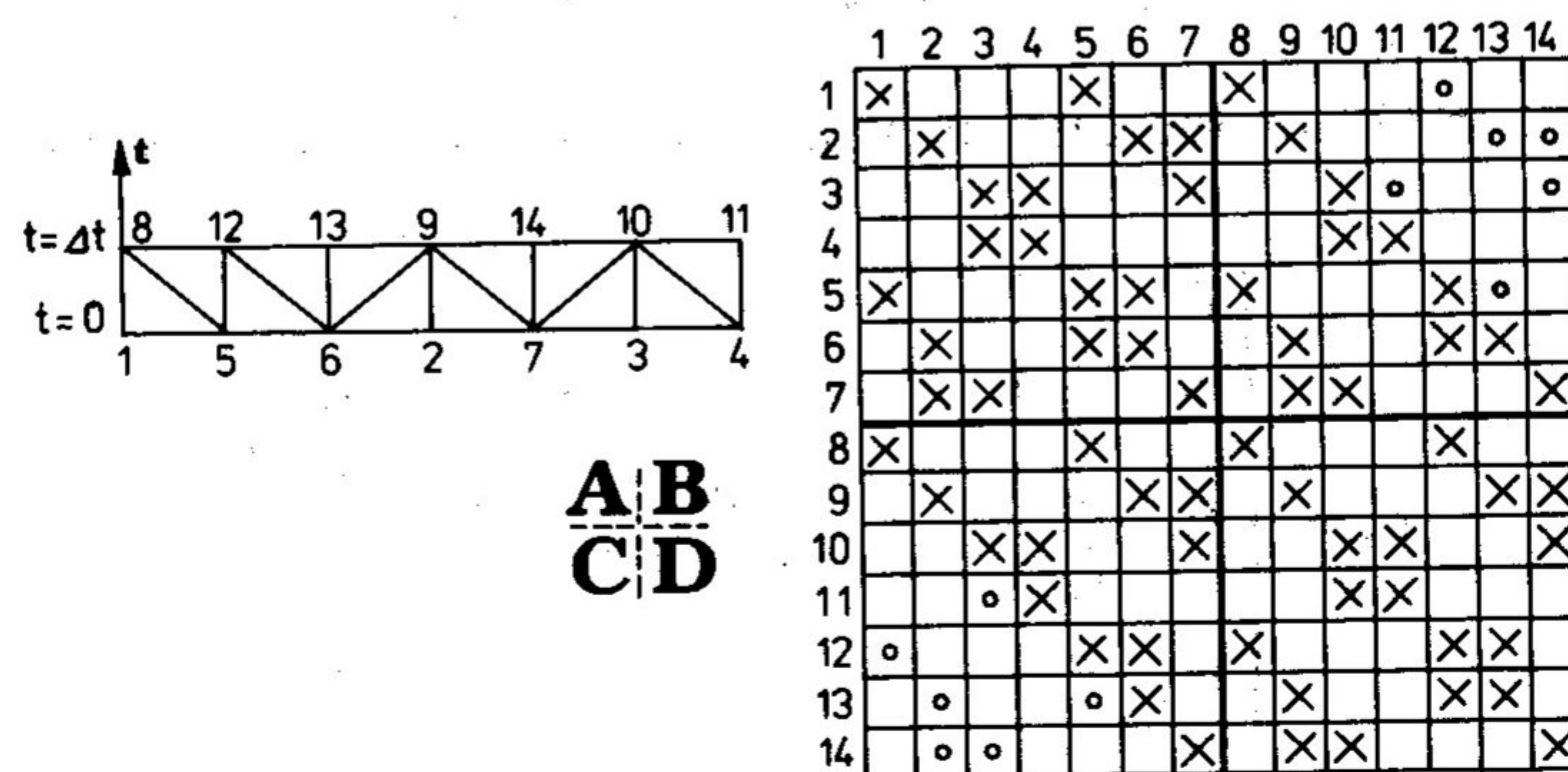


Figure 3. Example space-time net and its global matrix

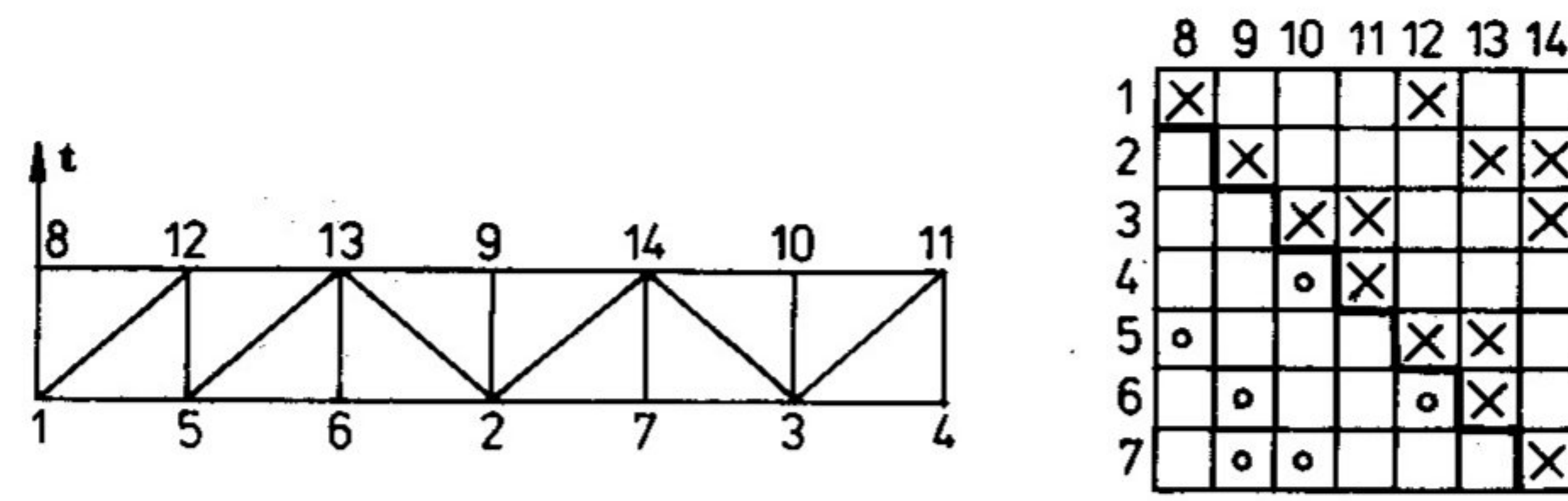


Figure 4. Space-time layer division and the triangular matrix of coefficients

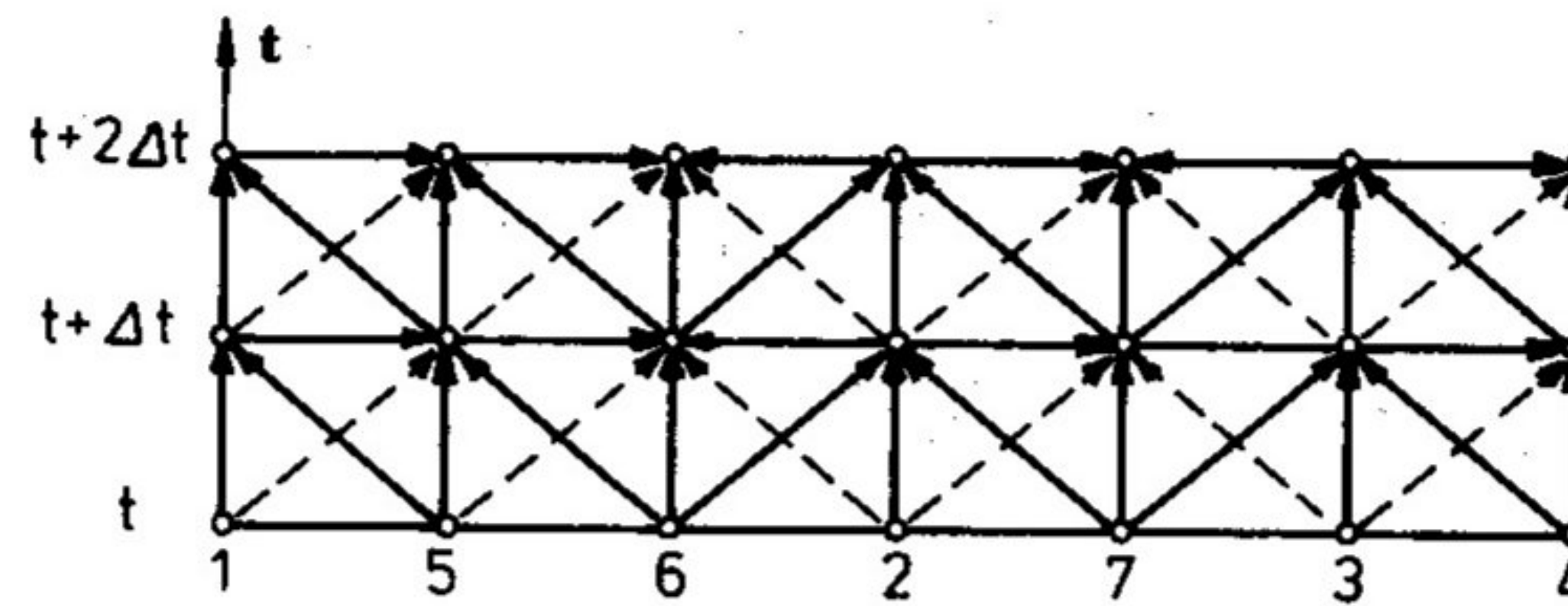


Figure 5. Information flow in the space-time element method

hand upper quarter of the global matrix denoted by **B** is a lower triangular matrix. We notice that the upper triangular form can also be obtained by a special space-time layer division into triangular elements (Figure 4). Now joint-by-joint solution must be started from the last node. Any other numeration and any space-time layer division are available but in that case joints must be analysed in a respective sequence. The analysis of the matrix shown in Figure 2 together with the system of space-time elements enables the investigation of the information flow among joints in the space-time layer (Figure 5). The form of the diagram depicted in Figure 5 is similar to the diagrams presented in Reference 5. Continuous lines denote the directions of the information flow which coincide with the element edges.

Anyway, as mentioned previously, the numbering of the nodes and the time layer partition are arbitrary. To simplify the computational algorithm a special method of space-time element generation was assumed. All nodes of the spatial division net are successively considered. Let the number of the considered joint be denoted by *i*. The space-time mesh can be simply constructed by the analysis of the mesh topology. All the joints connected with the joint *i* must be taken and if the joint number is greater than *i*, its time co-ordinate $t = 0$. In the case when it is less, its time co-ordinate $t = \Delta t$. Joint *i* gives two nodes at which $t = 0$ and $t = \Delta t$. The described method of space-time mesh generation in the case of surface structure is shown in Figure 6. The global matrix related to one space-time layer is held in core in the form of a sequence of submatrices the dimensions of which are equal to the nodal number of degrees of freedom. The constructed sequence of joint numbers neighbouring the successive joints serves as a pattern of submatrix location in the sequence of submatrices. The method of global matrix recording is presented in Figure 7. The sequence of submatrices shown in Figure 5 contains a number of zero blocks (denoted by points). They can be easily eliminated using the remark that if the joint number in the row of the surrounding number sequence is greater than *i* (underlined in Figure 7) the zero block is located at the first position. But, if the joint number in the row is less than *i*, the zero block appears in the third position. In the case of equality of the numbers the zero blocks do not appear.

The presented method of matrix recording ensures the entire exploitation of the memory. It is also essential that triangular matrices already require a smaller area of the memory. Based on the method presented the computer program was worked out. It was written in Fortran IV and was designed for any type of computer. It can be applied without modification in the

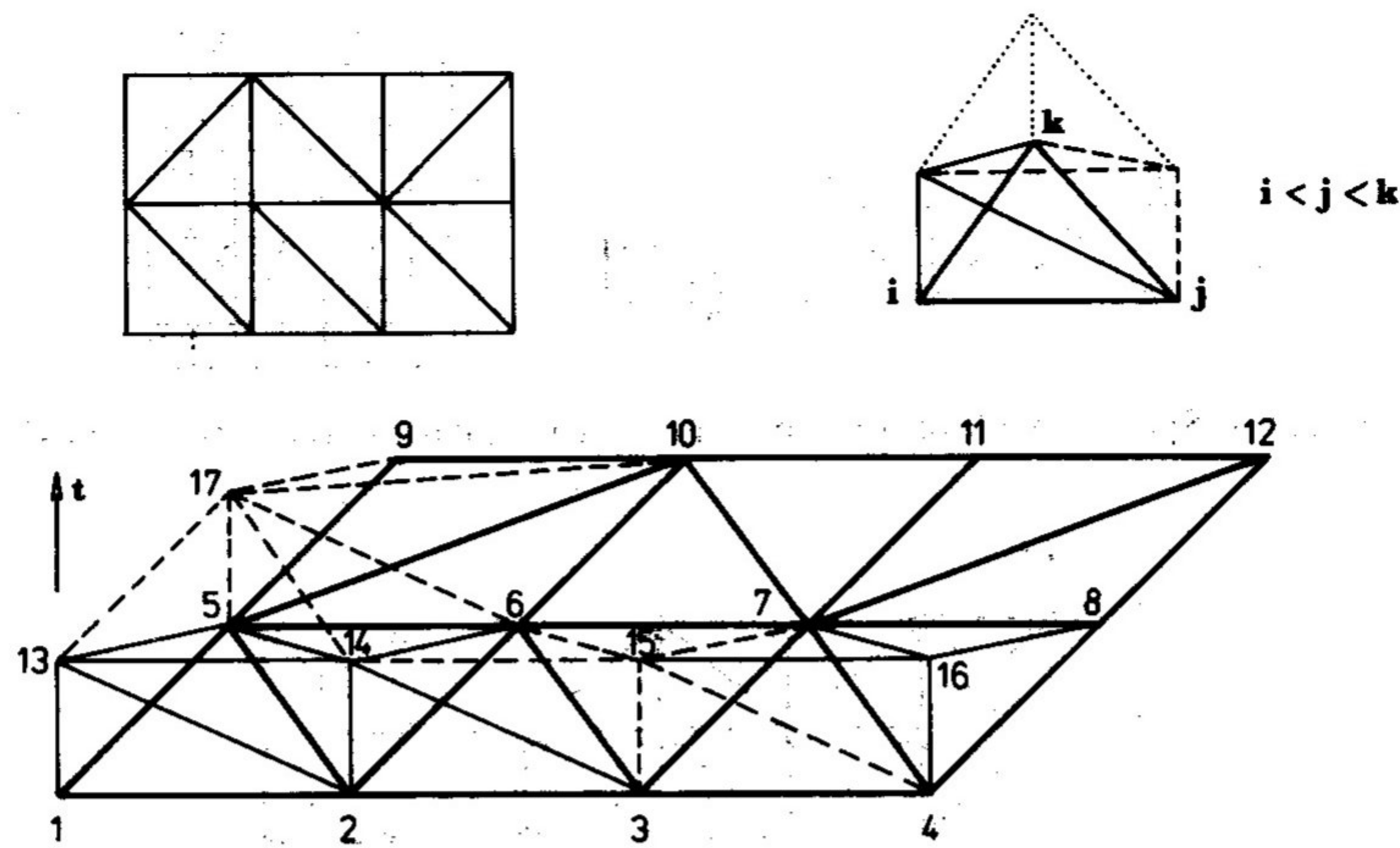


Figure 6. Space-time layer division into tetrahedral elements

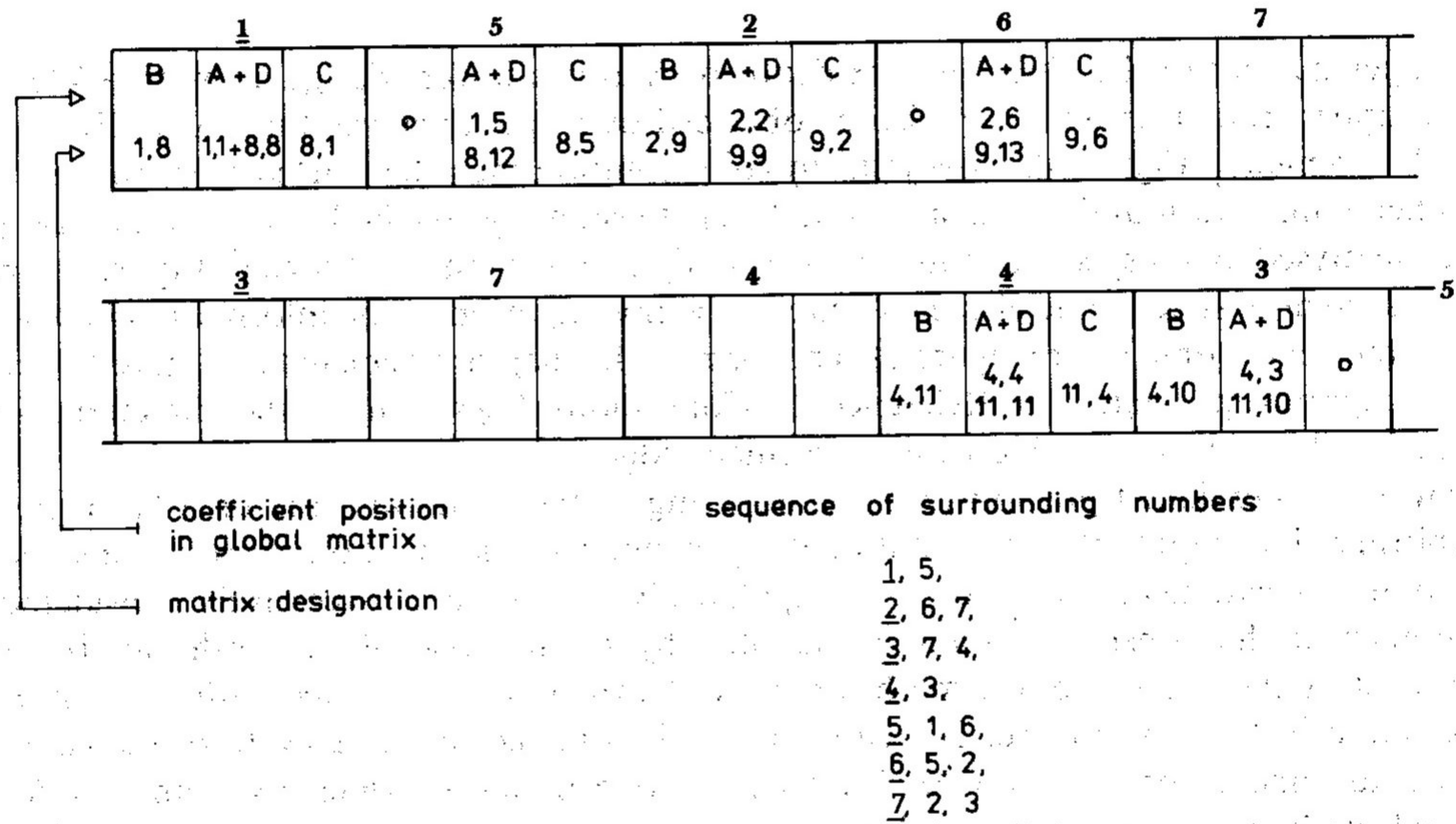


Figure 7. The disposition of matrices A, B, C and D in the memory for the example from Figure 3

dynamic analysis of any type of structure: beams, plates, three dimensional blocks and any higher problems of computational physics. A table whose dimension is declared at the top of the program is the only one that should be adjusted to the size of the available computer memory.

Analysis of the in-core storage efficiency

To evaluate the occupation of the memory by the matrices defined in the program, the number of words necessary in the example problem computation was estimated. In further considerations the word is understood as the number of machine words which represent a real number in the computer. As an example, a plate divided into 128 triangular elements was considered (Figure 8). To initiate the program a vector of 12,000 real numbers is required. The number of words

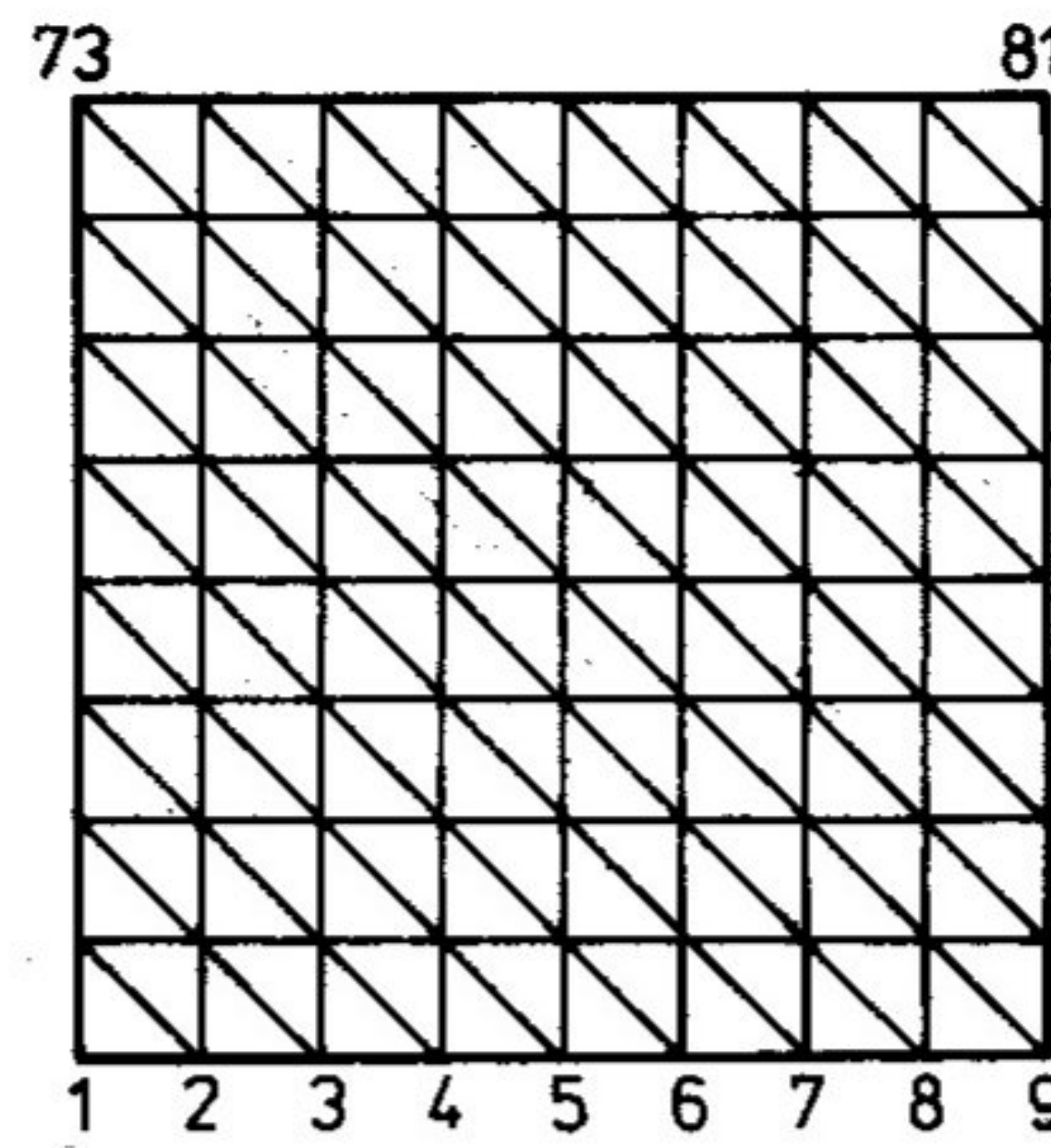


Figure 8. The net of the plate division

necessary to hold the global matrices of the system of equations was also evaluated. If n denotes the number of joints on the edge of the square mesh and s denotes the number of nodal degrees of freedom, the total memory used by the space-time stiffness matrix (measured in real numbers) is $(15n^2 - 16n + 4)s^2$ and the number of multiplications per time step is the same.

Remarks on the use of the external memory

In the case when the dimension of the problem enables the computations to be performed it is possible to use the version of the program collaborating with the random access external store. The global matrix, written in the form of submatrices, is held in the external store in several records. The program possesses a table which acts as a buffer in which one of the recorded parts of the global matrix is held. In computations two stages of exploitation of written matrices can be separated. In the first one the global stiffness matrix is formulated by addition of corresponding elements of local matrices. The formulation is carried out element by element, and hence some transmissions are inevitable in cases when element matrix coefficients hit the fields of different records. In the second stage displacements of joints at successive moments are computed. The reading of records is carried out sequentially. Interchange between the internal store buffer and the external store is optimum. In spite of the high efficiency of computations performed by the described procedure it can be applied only in special cases and under the condition of a large capacity of the buffer to reduce the number of transmissions at each step. Otherwise, the computations will last a long time by reason of transmissions only.

APPLICATIONS

It is interesting to compare the results obtained by the space-time finite element method and different element models with the exact solutions. Usually the simple oscillator with one degree of freedom was used in the investigations of previously constructed methods of time integration. Here more complicated schemes of structures have to be taken. Conventional methods of time integration allow one to separate the spatial dimensions from the time variable and in this way to obtain integration schemes independent of the finite element models. The STFEM enables the separation of the time variable and that is why the solution scheme accuracy is affected by the space-time element formulation. However, it is possible to obtain a one degree of freedom scheme.

Let us consider a bar in axial vibrations. Let the bar be modelled by one spatial finite element, one end of which is fixed. The space-time layer must be composed of two triangular space-time finite elements. Stiffness and mass matrices related to the movable end are

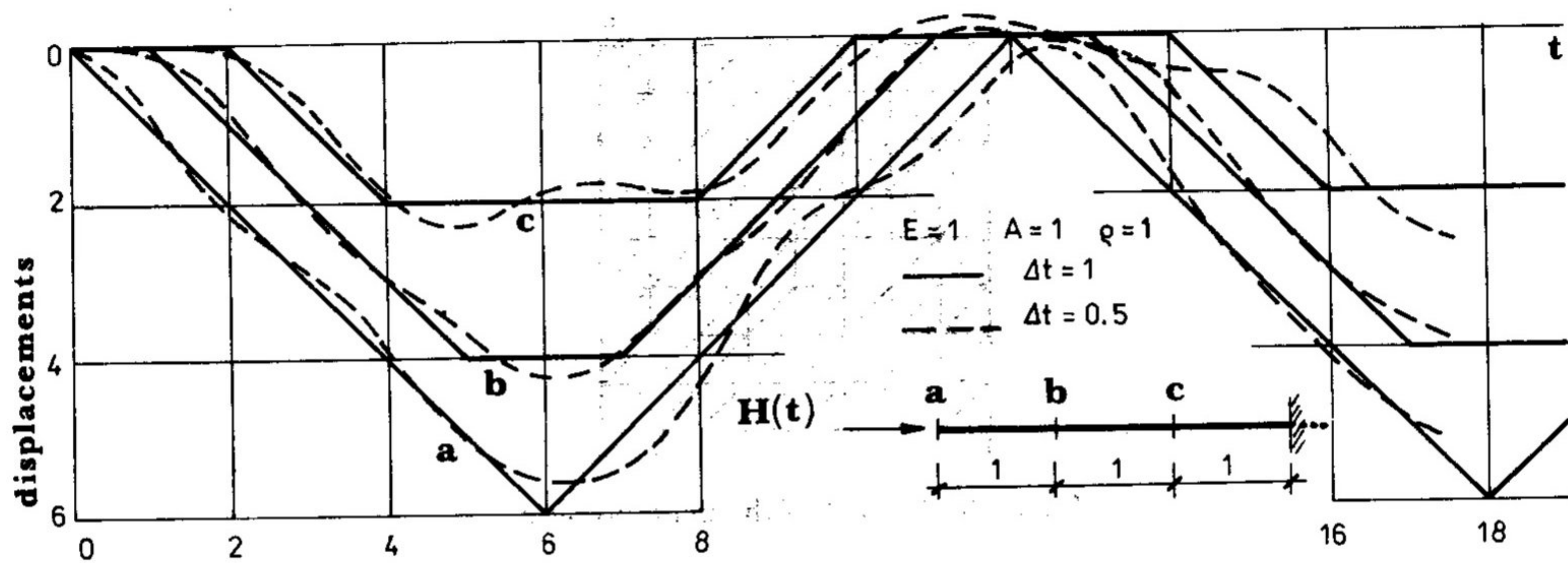


Figure 9. Displacements in time of a bar in axial vibration (triangular elements)

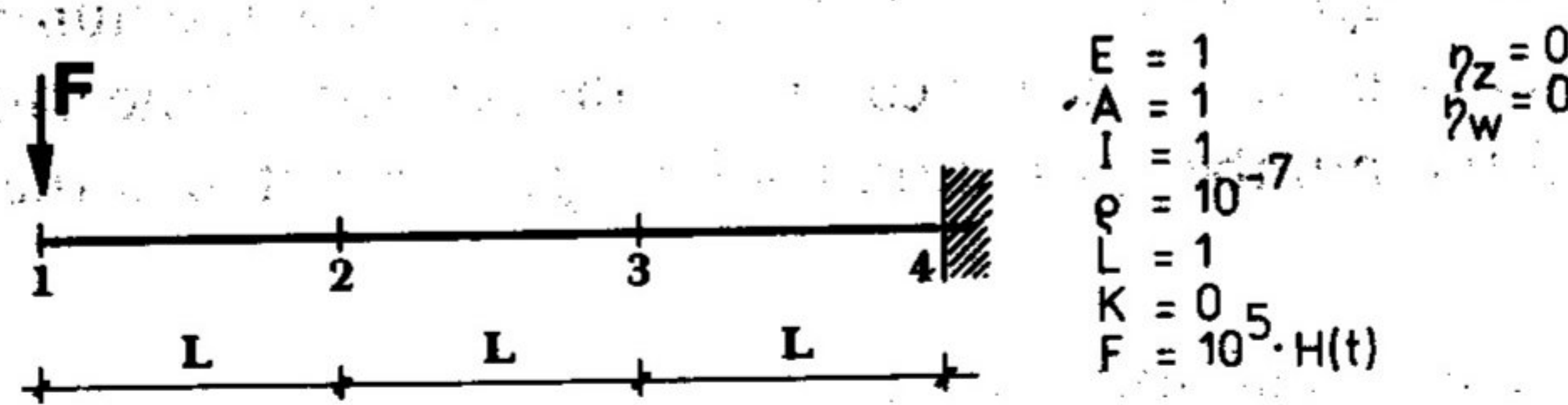


Figure 10. The tested problem

$$K = \frac{EAh}{2a} \begin{bmatrix} 1 & 0 \\ 0 & 1 \end{bmatrix}, \quad M = \frac{\rho Aa}{2h} \begin{bmatrix} 1 & -1 \\ -1 & 1 \end{bmatrix} \quad (47)$$

where a is the length of the bar element and h is the time step.

The equilibrium equation written for one moment leads to the recursive scheme

$$\begin{bmatrix} \frac{\rho Aa}{2h} & \frac{EAh}{a} & -\frac{\rho Aa}{h} & \frac{\rho Aa}{2h} \end{bmatrix} \begin{Bmatrix} \delta_{i-1} \\ \delta_i \\ \delta_{i+1} \end{Bmatrix} = F_i \quad (48)$$

where δ_i is the displacement at moment i and F_i is the nodal impulse at moment i , or

$$\delta_{i+1} = 2 \left(1 - \frac{c^2 h^2}{a^2} \right) \delta_i - \delta_{i-1} + \frac{2hF_i}{\rho Aa} \quad (49)$$

or

$$c = \sqrt{\left(\frac{E}{\rho} \right)}$$

The time step limitation

$$\frac{c^2 h^2}{a^2} < 2 \quad (50)$$

results from the stability analysis. For $c^2 h^2 / a^2 = 1$ and $F_i = h$ (let the Heaviside function describe the load) we obtain the sequence of displacements at successive moments: 0, 0.5, 1, 0.5, 0, 0.5, 1, ... (multiplier = $2h^2 / \rho Aa$). The period $T = 4a/c$ and the amplitude is $2a/EA$. We can see that accurate results were achieved. In the case $c^2 h^2 / a^2 = 0.5$ the successive displacements are 0, 0.5, 1.5, 2, 1.5, 0.5, 0, 0.5, ... so we have a phase error of 0.06 and accurate amplitude. Displacements in time of the bar split into three spatial elements are shown in Figure 9.

Triangular elements of a beam were used in the solution of the problem shown in Figure 10. $H(t)$ is the Heaviside function. The amplitude of joint 1 and the period of oscillations for both

Table I. Comparison of results in beam vibration analysis

Time step $\Delta t/\Delta t_{cr}$	First model		Second model		Exact value	
	A	T	A	T	A	T
0.1	1.6×10^6	69.0×10^{-4}	1.80×10^6	74.5×10^{-4}	1.8×10^6	51.0×10^{-4}
1.0	1.6×10^6	67.0×10^{-4}	1.80×10^6	74.0×10^{-4}	1.8×10^6	51.0×10^{-4}

A = amplitude, Δt = time step
 T = period of vibrations, Δt_{cr} = critical time step

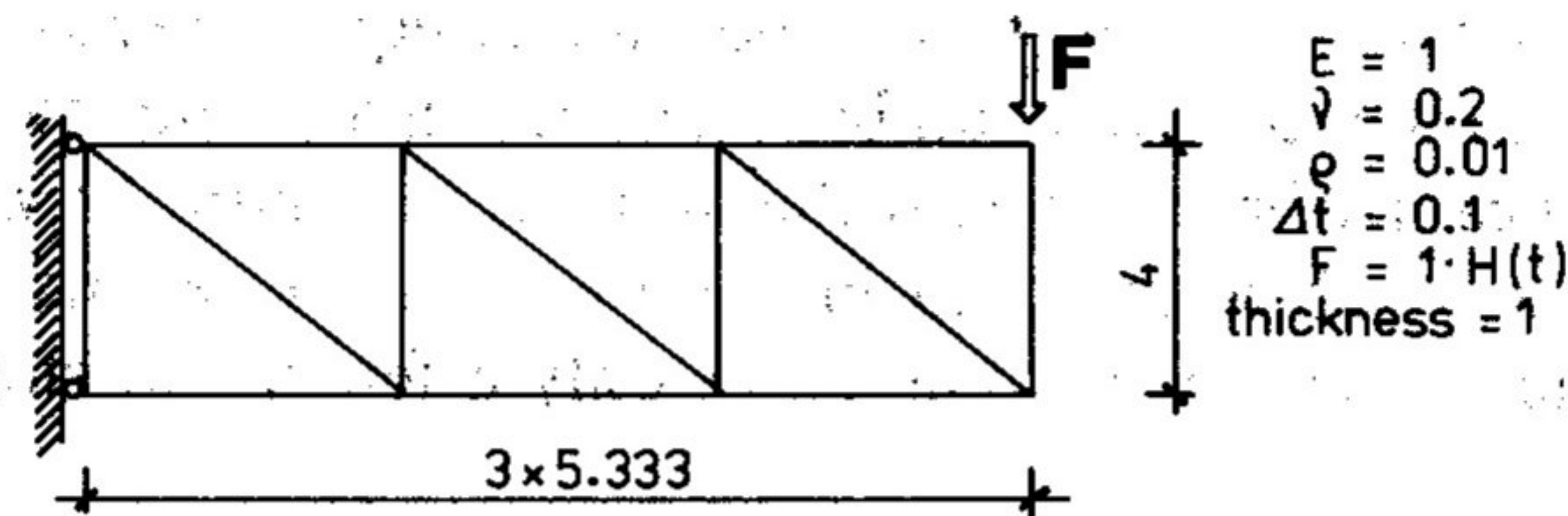


Figure 11. Plane stress analysis example.

models of triangular beam elements were compared with the exact values. Shear effects were neglected in computed examples. The results are gathered in Table I.

A similar test was performed for tetrahedral elements of plane stress analysis. A cantilever beam divided into 6 finite elements was considered (Figure 11). The amplitude of the subjected joint is 112, which is about 0.21 of the exact value. It must be noticed that the static solution of the same problem, in the case of constant stress elements, is also 0.21 of the exact value and in this example the method can be regarded as accurate.

Discussion of results

Although more complicated, even three-dimensional, problems were successfully solved, the simple tests presented above sufficiently exhibit the main properties of the method.

It can be noted that the amplitude error in all cases is neglectable. In axial vibrations of bars and beam vibrations with the use of the cubic model of STFE the amplitude results are accurate. The linear model of a beam element and, especially, tetrahedral elements of plane stress/strain endorse the influence of the precision of the element model formulation on the results.

The phase error is significant in some cases if compared with the exact solutions. It is worth quoting here some results from Reference 14. For different parameters $\beta \in [0, \frac{1}{2}]$ the period error of Newmark's method was investigated. The error was evaluated as a function of Δt . When the time step was equal to 0.25 of the period T it extended from 0.18 for $\beta = \frac{1}{4}$ to 0.43 for $\beta = \frac{1}{2}$. In a conditionally stable case ($\beta < \frac{1}{4}$) the respective values were 0.08 ($\beta = \frac{1}{6}$) and -0.13 ($\beta = 0$). The phase error comparison for other methods was described in Reference 5 and, also, its considerable values were exhibited. In this context the space-time triangular and tetrahedral elements can be accepted. It must be emphasized that the FEM is free of numerical (spurious) damping.

The space-time finite element method must be considered together with the space-time elements. It can be regarded as an extension of the FEM over the time domain and its properties depend on the element properties.

More general remarks

The space-time layer division into triangular and tetrahedral elements needs special discussion. The triangular space-time net shown in Figure 12 effects a flow of information with a speed not greater than the slope of the edges. The numbering, as in Figure 12, involves the anisotropy of the mathematical model. A similar problem has appeared in the Trujillo method⁴ and was discussed in Reference 5. But in the Trujillo method the direction of anisotropy is changed in successive time layers and in two steps the information is transmitted to all nodes. In the method described in this paper, the same effect can be obtained if the sequence of joint numbers in each second layer is changed. However, for the sake of storage minimization, another method was assumed. The successful numbering of each second joint in the spatial structure increases the limit of the speed of information flow twice and causes equal speeds in the two directions (Figure 13). To check the influence of the numbering on the final results two simple test problems were solved. Cantilever beam vibrations with the mesh as in Figure 12 were considered. In the first case the first joint was subjected to an impulse and in the second case the last one was forced. In both cases the displacements differed at only a few initial steps. After several steps the results coincided.

Non-linear problems can also be solved by the method described in this paper. The computational program must be modified to hold additional matrices C_i and D_i for the $(i + 1)$ th layer of joints (14). Both of them take about 0.75 of the total memory desired for the linear

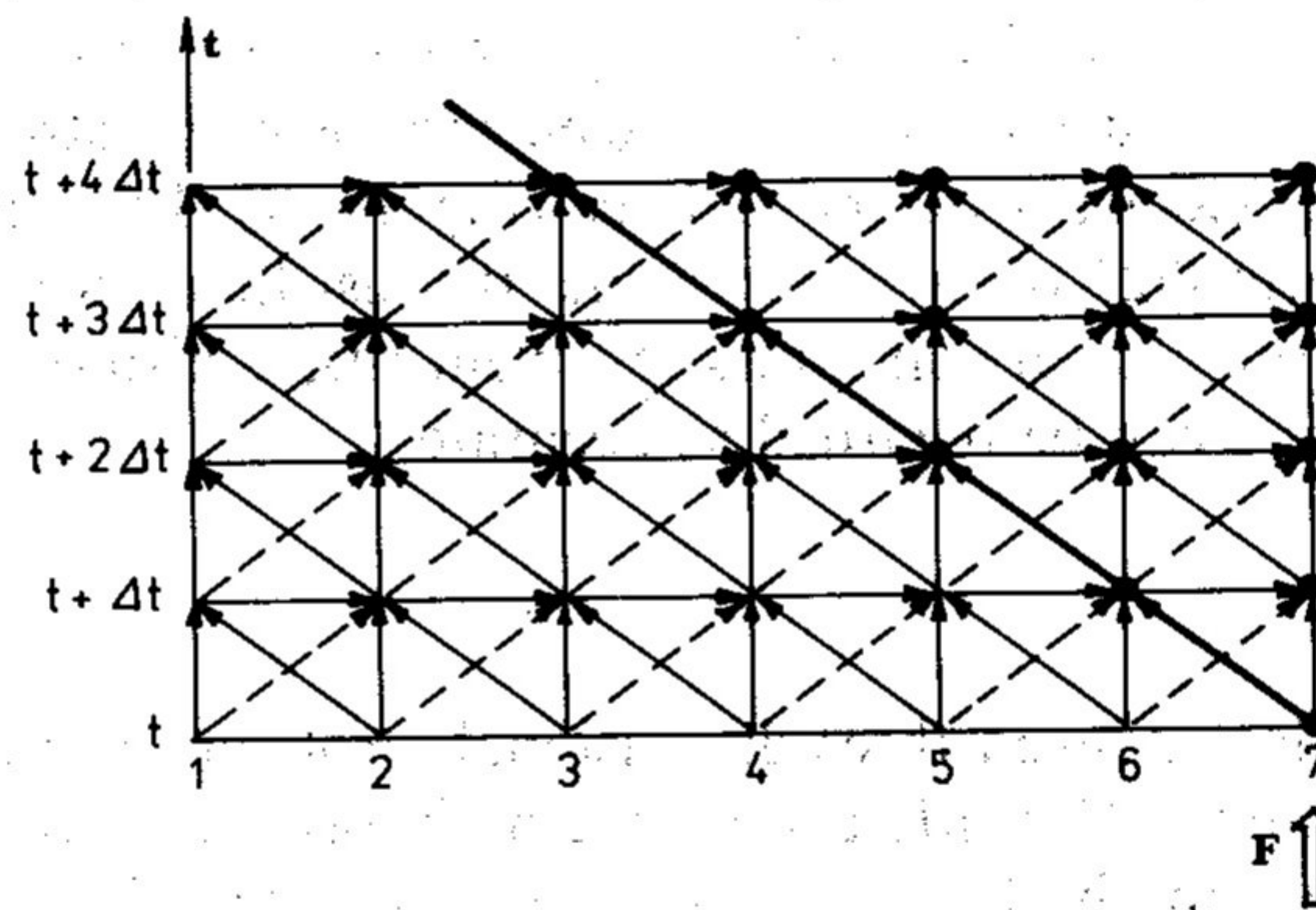


Figure 12. The information flow in the case of successive numbering

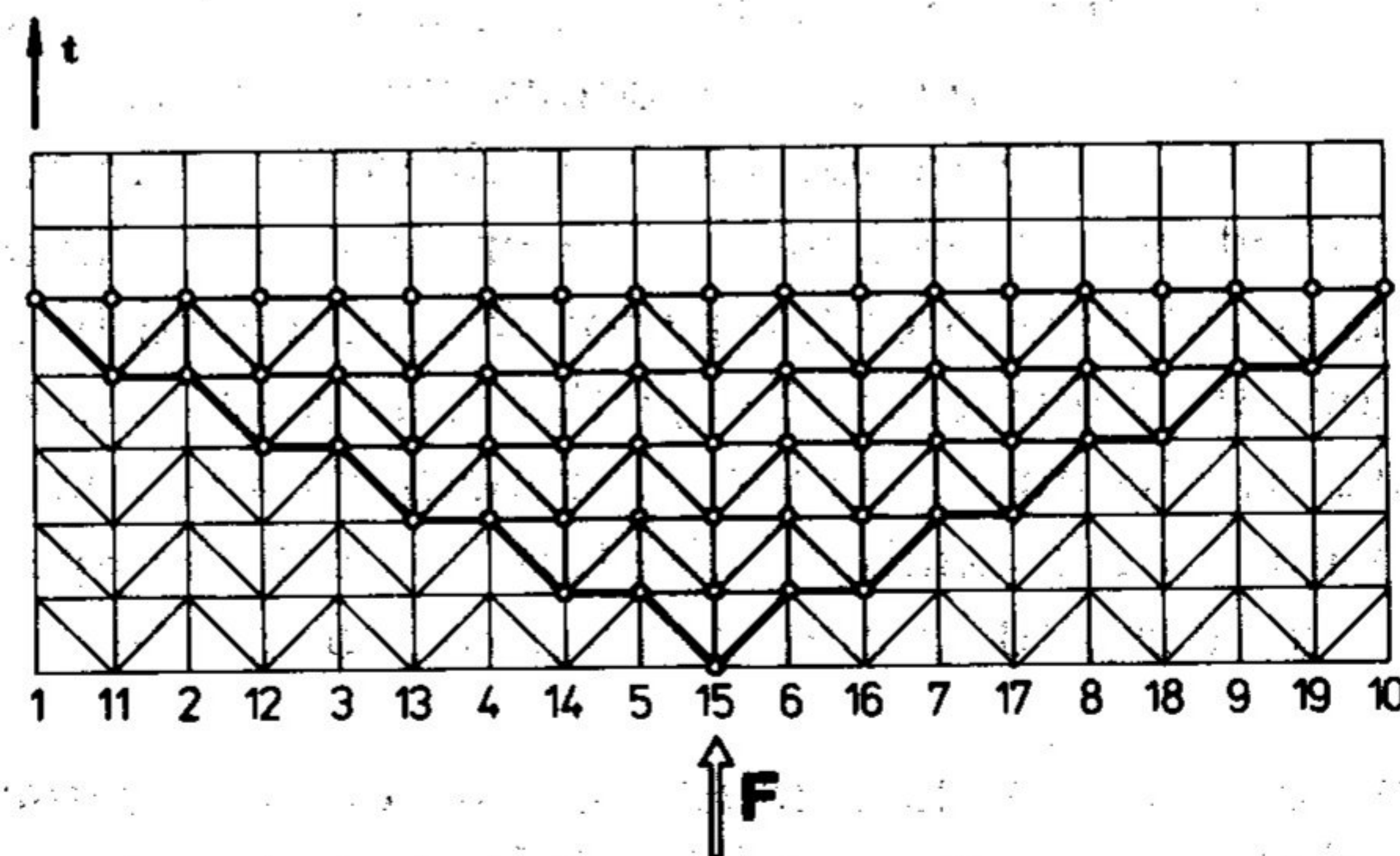


Figure 13. Isotropic information propagation

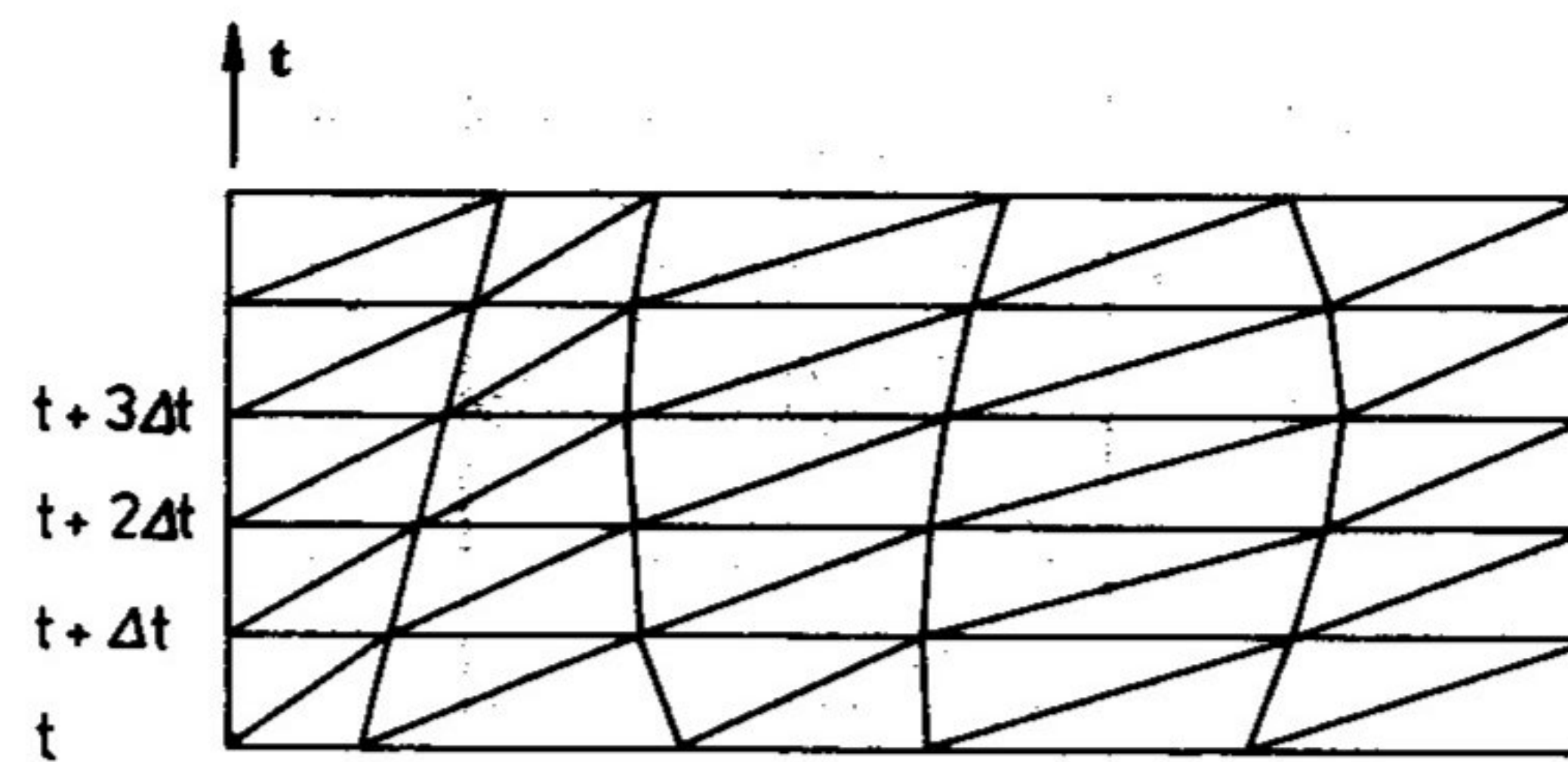


Figure 14. Non-stationary division of a beam

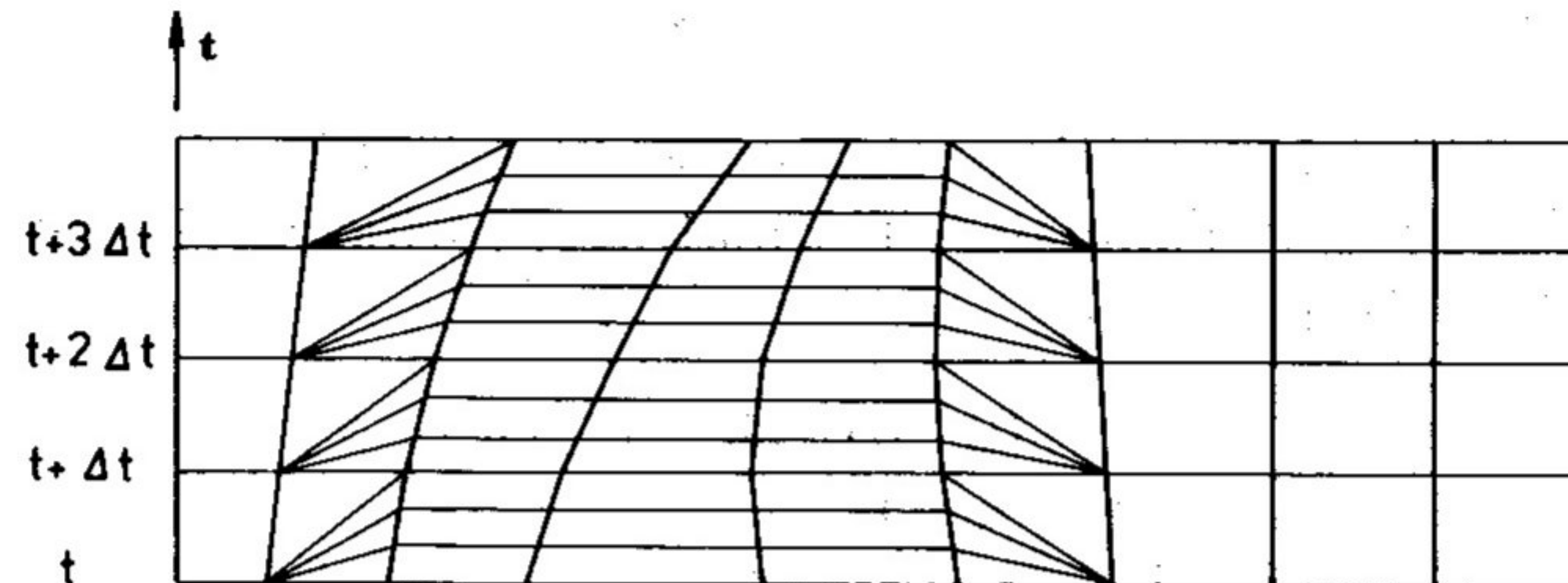


Figure 15. Time division condensation in some regions of the structure

problem. Non-linearity can be of two types. Non-linear material properties in elastic-plastic problems, the influence of the unilateral elastic foundation and other contact problems can be of the first type of non-linear analysis. The second type is when a non-stationary division of the structure into finite elements is assumed¹⁵ (Figure 14). Non-stationary time-space partition was used in dynamic analysis of a beam placed on a unilateral foundation.¹⁶ The time-space partition was adjusted to the soil-structure contact area. The space-time element edges were always in coincidence with the lines limiting the contact zone. Moreover, triangular space-time elements were used in the time division condensation in regions of high stiffness of the structure (Figure 15). To complete the information included in this paper it should be emphasized that the stability limitations have to be considered. Two cases of non-stationary division can be determined in which the stability restrictions limit the size and the shape of the elements. The first case is when the time-space layer is divided into triangular elements, but the joint locations at the bottom and the top of the time layer are the same. Here the time step is the only factor which limits the application of the triangular elements. The second case is more general. The joint locations at two successive moments are changed (Figure 14). The limitations depend on the time step on one hand and on the speed of joint dislocation on the other hand. Since the simple investigation for one degree of freedom could not be applied, more complicated reproducible systems of elements were used in examinations.

STABILITY ANALYSIS

In the application of the space-time FEM two reasons for instability can be indicated. The value of the time dimension of the elements, i.e. the time step, is the first one. In the case of non-rectangular STFES it is difficult to express analytically the influence of the time step on the stability of computational schemes. The time variable is mixed with the spatial variables and cannot be separately observed. For each type of STFE model a new investigation process must be carried on. The problem is wide and can be properly shown only in a separate paper. A short introduction into the way of the testing and some practical conclusions can be cited in the paper.

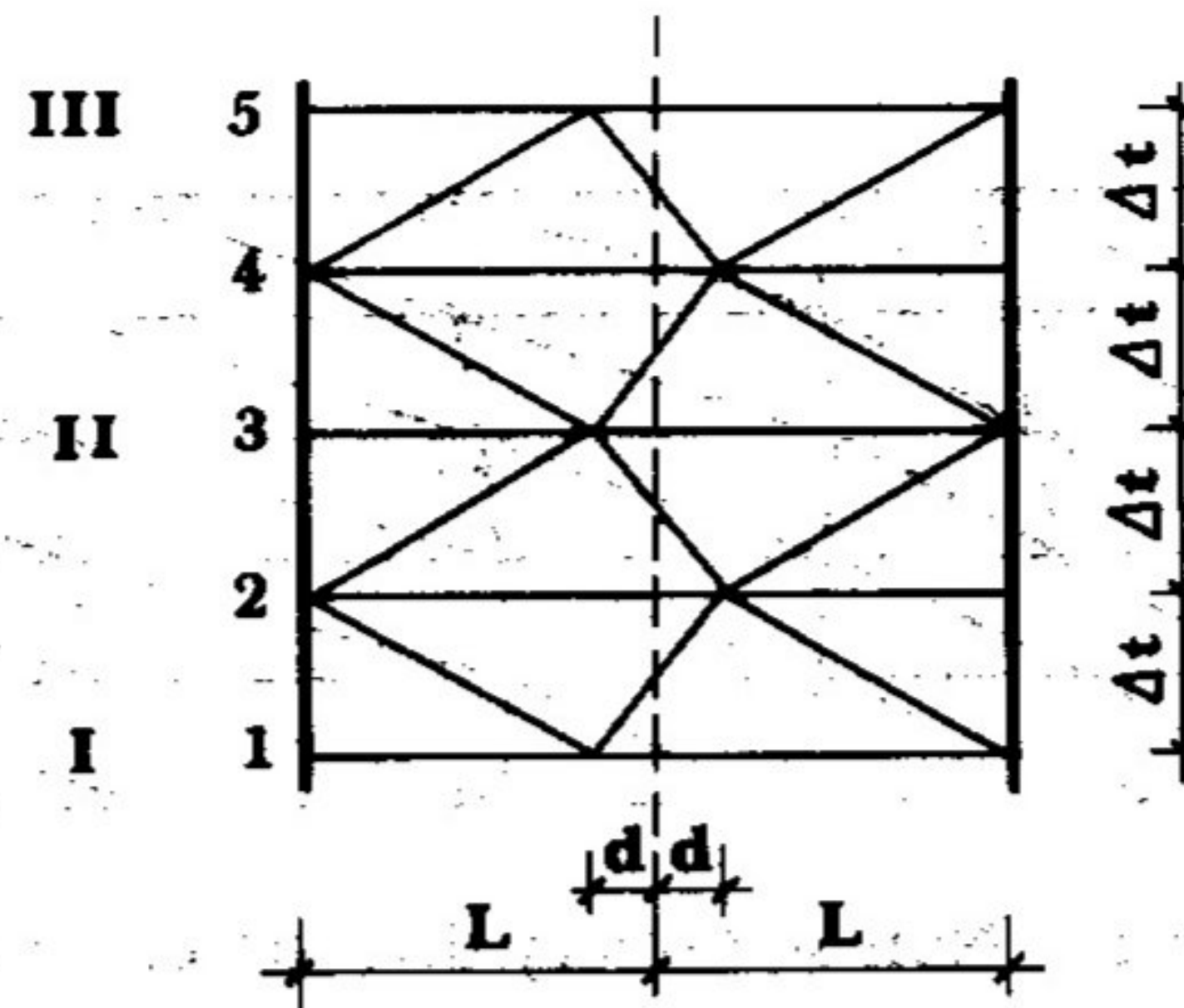


Figure 16. Space-time band used in stability analysis

In the case of a beam a separated part of a space-time half band is depicted in Figure 16. Every second layer of nodes was eliminated. The matrix of coefficients of the system of equations can be written in a block form:

$$\begin{bmatrix} \mathbf{F} & \mathbf{A} & \mathbf{B} & & \\ & \mathbf{C} & \mathbf{D} & \mathbf{E} & \\ & & \mathbf{F} & \mathbf{A} & \mathbf{B} \\ & & & \mathbf{C} & \mathbf{D} & \mathbf{E} \end{bmatrix}$$

For free vibrations an equation of the step-by-step procedure is obtained:

$$(-\mathbf{F}\mathbf{D}^{-1}\mathbf{C})\delta_I + (\mathbf{A} - \mathbf{F}\mathbf{D}^{-1}\mathbf{E} - \mathbf{B}\mathbf{D}^{-1}\mathbf{C})\delta_{II} + (-\mathbf{B}\mathbf{D}^{-1}\mathbf{E})\delta_{III} = \mathbf{0} \tag{51}$$

The same can be written by the use of the amplification matrix \mathbf{T} :

$$\begin{Bmatrix} \delta_{i+2} \\ \delta_i \end{Bmatrix} = \mathbf{T} \begin{Bmatrix} \delta_i \\ \delta_{i-2} \end{Bmatrix} \tag{52}$$

where

$$\mathbf{T} = \begin{bmatrix} (\mathbf{B}\mathbf{D}^{-1}\mathbf{E})^{-1}(\mathbf{A} - \mathbf{F}\mathbf{D}^{-1}\mathbf{E} - \mathbf{B}\mathbf{D}^{-1}\mathbf{C}) & -(\mathbf{B}\mathbf{D}^{-1}\mathbf{E})^{-1}\mathbf{F}\mathbf{D}^{-1}\mathbf{C} \\ \mathbf{I} & \mathbf{0} \end{bmatrix} \tag{53}$$

\mathbf{I} is the unitary matrix and $\mathbf{0}$ is the zero matrix. The stability condition in the problem (52) is described in References 17 and 18. If the spectral radius Ψ of the matrix \mathbf{T} is less than one:

$$\Psi(\mathbf{T}) < 1 \tag{54}$$

the recurrence scheme (51) is stable. In the case of $\Psi(\mathbf{T}) = 1$, when the radius is multiple root of the characteristic equation, the problem (51) is also unstable. Below some conclusions for triangular and tetrahedral elements will be presented.

According to Figure 16 two dimensionless coefficients will be introduced. The first one represents the time step Δt related to the critical value Δt_{cr} :

$$z = \frac{\Delta t}{\Delta t_{cr}} \tag{55}$$

The second one describes the speed of joint dislocation compared to the speed of wave propagation in the elastic medium

$$\xi = \frac{d}{\Delta t} \frac{1}{\sqrt{\left(\frac{E}{\rho}\right)}} \tag{56}$$

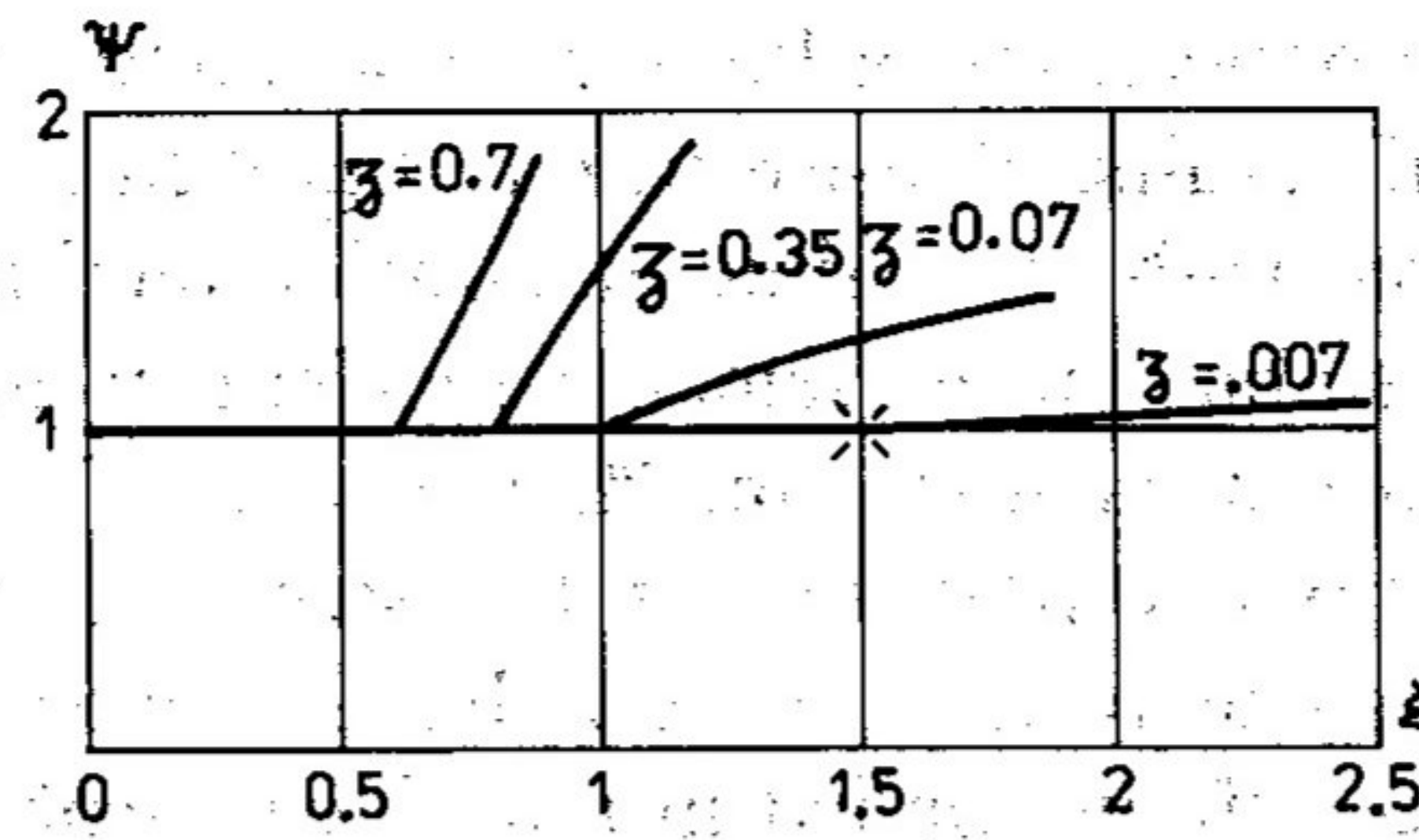


Figure 17. Triangular beam element (second model)—stability condition

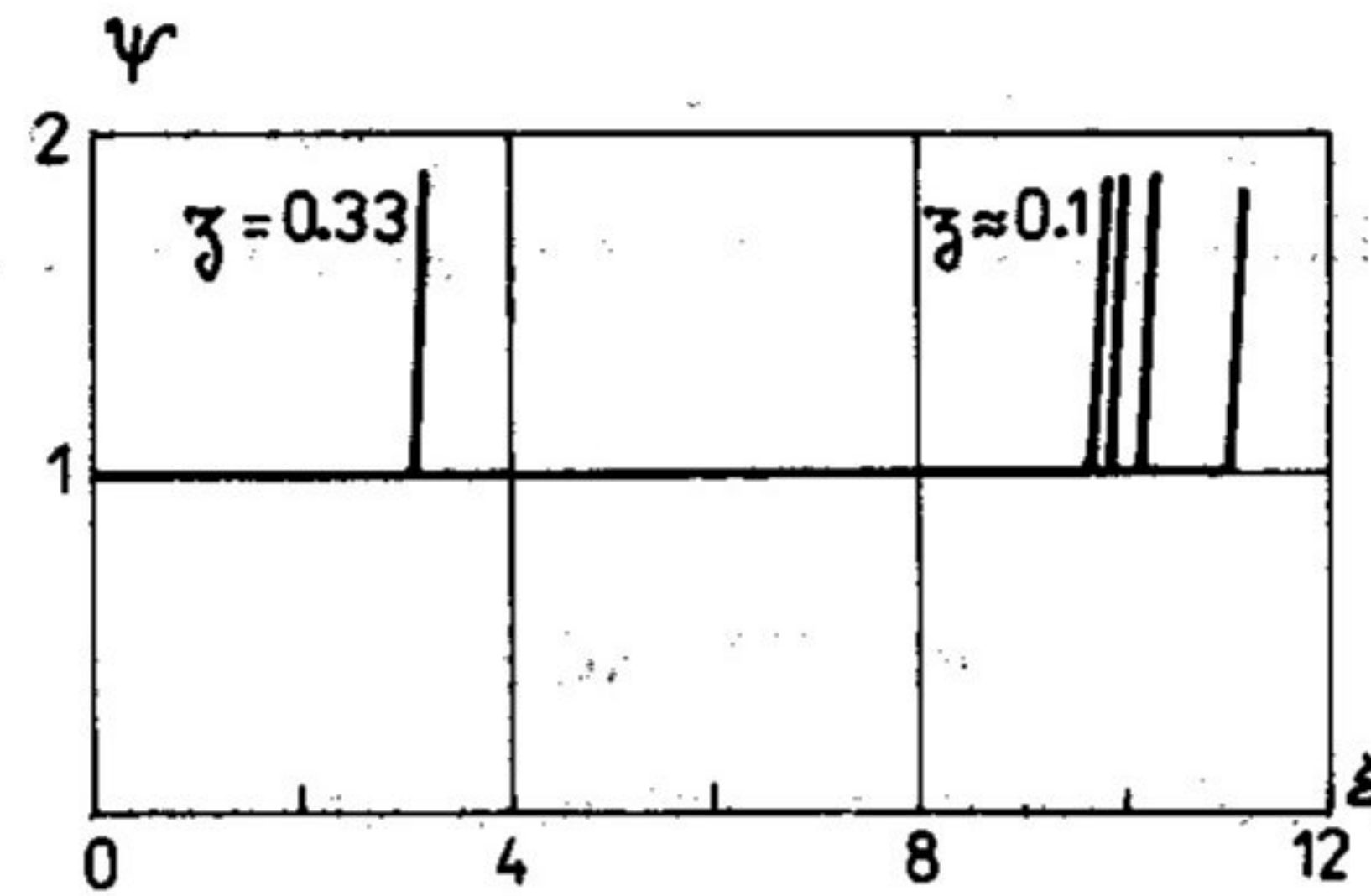


Figure 18. Tetrahedral element of plane stress/strain—stability condition

The spectral radius Ψ can be depicted in terms of the value ξ (Figures 17 and 18). It can be seen that in the case of beam elements the critical value of $\xi = 1.5$ was obtained. An identical result was obtained for the quadrangular space-time beam element.¹⁴ The plane stress/strain element has poor stability properties. The range of ξ which ensures the stable oscillations is not coherent. It makes application of such an element difficult. Considering the impossibility of inclusion of the internal damping (45) the new model of higher polynomial order should be introduced.

The time step for triangular elements of a bar is limited by the value

$$h \leq \sqrt{2} \frac{b}{c} \quad (57)$$

where b is the length of a spatial element and c is the wave speed, whereas in the case of rectangular bar elements the same condition is

$$h \leq 2 \frac{b}{c} \quad (58)$$

The limits of the parameter ξ in the cases of triangular and quadrangular bar elements are

$$\xi \leq \sqrt{2} \quad (59)$$

and

$$\xi \leq \sqrt{3} \quad (60)$$

respectively.

CONCLUSIONS

The accuracy of the STEFM with the use of simplex-shaped elements described in the paper strongly depends on the quality of the space-time element, in the meaning of its mathematical model. Amplitude error is neglectable when comparing results not with the theoretical value

but with FEM calculations. Imperfections of finite elements and space-time finite elements are of great influence on the final results. Phase error is significant if compared with analytical calculations but, when compared with other time integration methods, the accuracy is sufficient. The method is conditionally stable. Improvements in element formulation may lead to the unconditionally stable formulation as was done in the case of rectangular, multiplex-shaped elements. Comfort in non-stationary partition of the structure makes the method useful in engineer's practice. Although some restrictions on the time-space division are imposed, the approach described can be successfully applied in non-linear problems.

Triangular, tetrahedral and hyper-tetrahedral space-time elements lead to a lower triangular matrix of coefficients in the system of equations. A special algorithm ensures high effectiveness in storage and in computations.

Many methods of time integration give an infinite speed of information flow that contradicts the reality. Here the speed of disturbance is limited and it improves the differential equation solution.

REFERENCES

1. T. Belytschko and R. Mullen, 'Stability of explicit-implicit mesh partitions in time integration', *Int. j. numer. methods eng.*, **12**, 1575-1586 (1978).
2. T. J. R. Hughes and W. K. Liu, 'Implicit-explicit finite elements in transient analysis: stability theory', *J. Appl. Mech.*, **45**, 371-374 (1978).
3. K. C. Park and C. A. Felippa, 'Partitioned transient analysis procedure for coupled-field problems: accuracy analysis', *J. Appl. Mech.*, **47**, 919-926 (1980).
4. D. M. Trujillo, 'An unconditionally stable explicit algorithm for structural dynamics', *Int. j. numer. methods eng.*, **11**, 1579-1592 (1977).
5. R. Mullen and T. Belytschko, 'An analysis of an unconditionally stable explicit method', *Comp. and Struct.*, **16**, 691-696 (1983).
6. K. C. Park and J. M. Housner, 'Semi-implicit transient analysis procedure for structural dynamics analysis', *Int. j. numer. methods eng.*, **18**, 609-622 (1982).
7. K. C. Park, 'Practical aspects of numerical time integration', *Comp. and Struct.*, **7**, 343-353 (1977).
8. O. C. Zienkiewicz, 'Finite elements in the time domain', in A. K. Noor and W. D. Pilkey (eds), *State-of-the-Art Surveys on Finite Element Technology*, ASME, 1983.
9. J. H. Argyris and D. W. Scharpf, 'Finite element in space and time', *Nucl. Eng. Design*, **10**, 456-469 (1969).
10. J. T. Oden, 'A general theory of finite elements—I: topological considerations, II: applications', *Int. j. numer. methods eng.*, **1**, 205-221, 242-260 (1969).
11. Z. Kączkowski, 'The method of finite space-time elements in dynamics of structures', *J. Techn. Physics*, **16**, 69-84 (1975).
12. Z. Kączkowski, 'General formulation of stiffness matrix for space-time finite elements', *Archiwum Inżynierii Lądowej*, **25**, 351-357 (1979).
13. Z. Kączkowski and J. Langer, 'Synthesis of the space-time finite element method', *Archiwum Inżynierii Lądowej*, **26**, 11-17 (1980).
14. Z. Kacprzyk and T. Lewinski, 'Comparison of some numerical integration methods for the equations of the motion of systems with a finite number of degrees of freedom', *Engineering Trans.*, **31**, 213-240 (1983).
15. C. I. Bajer, 'Non-stationary division by the space-time finite element method in vibration analysis', in M. Petyt and H. F. Wolfe (eds), *Proc. Second Int. Conf. on Recent Advances in Structural Dynamics*, Southampton 1984, pp. 161-170.
16. C. I. Bajer, 'Dynamic analysis of a beam placed on a unilateral foundation', *Ph.D. Thesis*, Politechnika Warszawska, Warszawa, 1983 (in Polish).
17. J. Legars, *Méthodes et de l'Analyse Numérique*, Dunod, Paris, 1971.
18. K. Bathe and E. Wilson, *Numerical Methods in Finite Element Analysis*, Prentice-Hall, New Jersey, 1976.